Journal of the Korean Magnetic Resonance Society **2020**, *24*, 117-122
DOI http://dx.doi.org/10.6564/JKMRS.2020.24.4.117

NMR Hydrogen Exchange Study of DNA Duplex Containing the Consensus Binding Site for Human MEIS1

Seo-Ree Choi, Ho-seong Jin, Yeo-Jin Seo and Joon-Hwa Lee*

Department of Chemistry and Research Institute of Natural Science, Gyeongsang National University, Jinju 52828, Republic of Korea

Received Dec 3, 2020; Revised Dec 17, 2020; Accepted Dec 17, 2020

Abstract Transcription factors are proteins that bind specific sites or elements in regulatory regions of DNA, known as promoters or enhancers, where they control the transcription or expression of target genes. MEIS1 protein is a DNA-binding domain present in human transcription factors and plays important roles in various biological functions. The hydrogen exchange rate constants of the imino protons were determined for the wild-type containing the consensus DNA-binding site for the MEIS1 and those of the mutant DNA duplexes using NMR spectroscopy. The G2A-, A3G- and C4T-mutant DNA duplexes lead to clear changes in thermal stabilities of these four consensus base pairs. These unique dynamic features of the four base pairs in the consensus 5'-TGAC-3' sequence might play crucial roles in the effective DNA binding of the MEIS1 protein.

Keywords NMR, DNA binding, Hydrogen exchange, MEIS1 transcription factor, Base-pair stability

Introduction

Transcription factors are proteins that bind specific sites or elements in regulatory regions of DNA, known as promoters or enhancers, where they control the transcription or expression of target genes. Myeloid ecotropic viral integration site-1 (MEIS1) was discovered because its overexpression, induced by retroviral integration in the Meis1 gene, leads to myeloid leukemia.[1,2] Random retroviral mutagenesis identified Meis1 among the oncogenic integration sites.[2,3] The frequent association of integration and overexpression of MEIS1 and HOXA9[4] generated aggressive murine and human leukemias (acute lymphoblastic leukemia),[1,4] Moreover, MEIS1 is highly expressed in ovarian cancer,[5] while in neuroblastomas the MEIS1 gene is amplified and overexpressed.[6] Finally, MEIS1 overexpression promotes cell proliferation and resistance to apoptosis.[7] Homeobox genes, of which the most well characterized category is represented by the HOX genes, play central roles in embryogenesis and differentiation. The 60 amino acids long homeodomain is atypical, characterizing the TALE (three amino acids loop extension) class that contains three extra amino acids between the first and the second α-helices.[8,9]

Recently, the DNA consensus sequence for MEIS1 binding was identified by systematic evolution of ligands by exponential enrichment (SELEX) or random binding site selection. The highly conserved DNA-binding TALE proteins is responsible for specific recognition of a common sequence motif, [5'-TGACA-3'].[10] To understand the DNA binding mechanism of MEIS1 protein, the imino proton exchange rates were measured for the DNA duplex

* Address correspondence to: **Joon-Hwa Lee,** Department of Chemistry and Research Institute of Natural Science, Gyeongsang National University, Jinju 52828, Republic of Korea, Tel: 82-55-772-1490; Fax: 82-55-772-1489; E-mail: joonhwa@gnu.ac.kr

containing the consensus DNA-binding site for the MEIS1 transcription factor (referred to as msDNA duplex, Fig. 1). To further understand the correlation between the base pair stability/dynamics and DNA binding affinity of the MEIS1, the exchange rate constants of the imino protons for the wt-msDNA duplex were compared with those of the mutant msDNA duplexes (*see* Fig. 1), which display different binding affinities for MEIS1 protein.

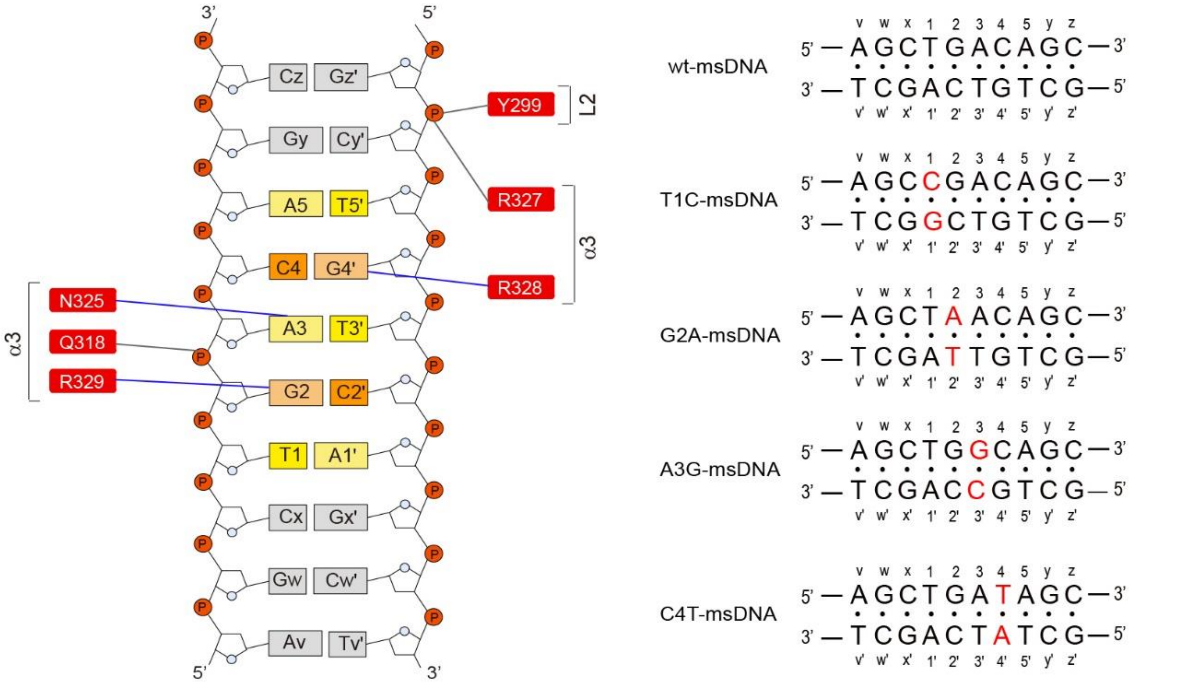

Figure 1. Residues of MEIS1 involved in intermolecular interaction with msDNA (left). DNA sequence contexts of the wt-, T1C-, G2A-, A3G-, and C4T-msDNA duplexes (right).

Experimental Methods

All DNA oligonucleotides were purchased from M-biotech Co. (Seoul, Korea). The oligonucleotides were purified and desalted by Sephadex G-25 column. DNA duplexes were dissolved in NMR buffer (90% H_2O/10% D_2O solution containing 10mM sodium phosphate (pH 6.0) and 100mM NaCl). NMR experiments were carried out on an Agilent DD2 700 MHz spectrophotometer (GNU, Jinju) equipped with a triple resonance probe. One-dimensional (1D) NMR data were processed and analyzed with the program Mnova 12.0.3 (Mestrelab Research, Spain) software and 2D data were processed with the program NMRPIPE[11] and analyzed with the program NMRFAM-Sparky.[12] To measure the hydrogen exchange rates of the imino protons, water magnetization transfer experiments [13] were performed using delay times ranging from 5 to 100 ms. The imino hydrogen exchange rate constants (k_{ex}) was determined by fitting the data to Eq. (1):

$$\frac{I(t)}{Io} = 1 - 2\,\frac{k_{ex}}{(R_{1w}-R_{1a})}\,(e^{-R_{1a}t} - e^{-R_{1w}t}) \qquad (1)$$

where R_{1a} and R_{1w} were the independently measured and are the apparent longitudinal relaxation rates of the imino proton and water, respectively, and I_0 and $I(t)$ are the peak intensities of the imino proton in the water magnetization transfer experiments at times zero and t, respectively. Hydrogen exchange experiment data were processed with the program Origin 2019.

Results and Discussion

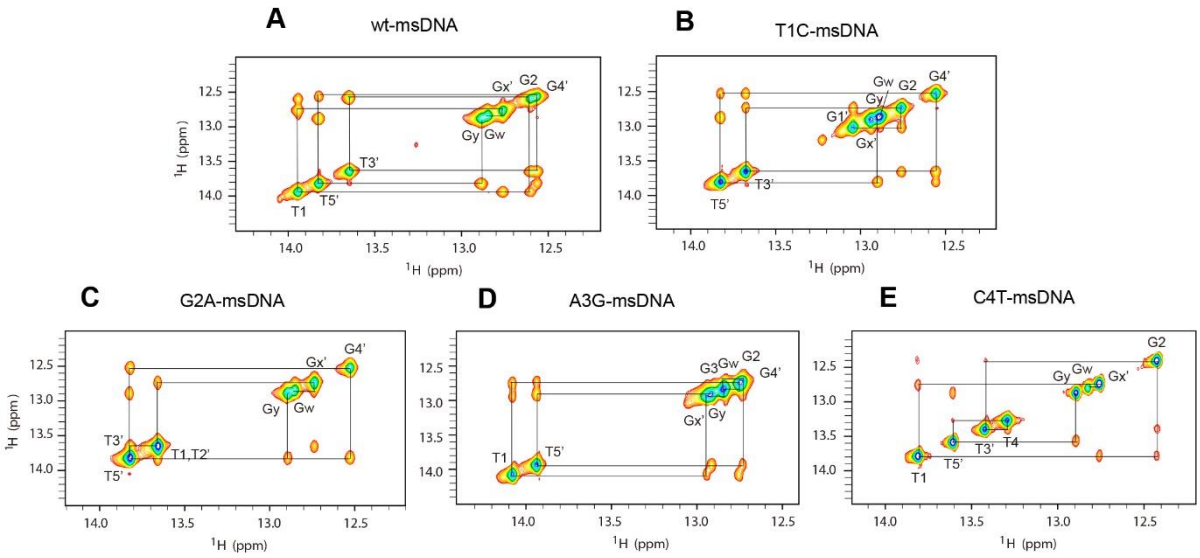

Figure 2. Expanded NOESY spectra (200 ms mixing time) contour plots of the wt- and mutant msDNA duplexes in 90% H_2O/10% D_2O NMR buffer at 5 ℃.

The resonance assignment of the 2D NOESY spectra of the wt-, T1C-, G2A-, A3G-, and C4T-msDNA duplexes in 90% H_2O/10% D_2O buffer solution containing 10 mM sodium phosphate (pH 6.0) and 100mM NaCl were acquired at 5 ℃ with 200 ms mixing times. The imino proton resonances were assigned by the strong G-imino to T-imino NOE cross peaks in the NOESY spectra (Fig. 2). Fig. 3 shows temperature-dependent imino proton spectra of the wt-, T1C-, G2A-, A3G- and C4T-msDNA duplexes. In all five duplexes, all imino proton resonances except terminal imino proton resonances could be observed at

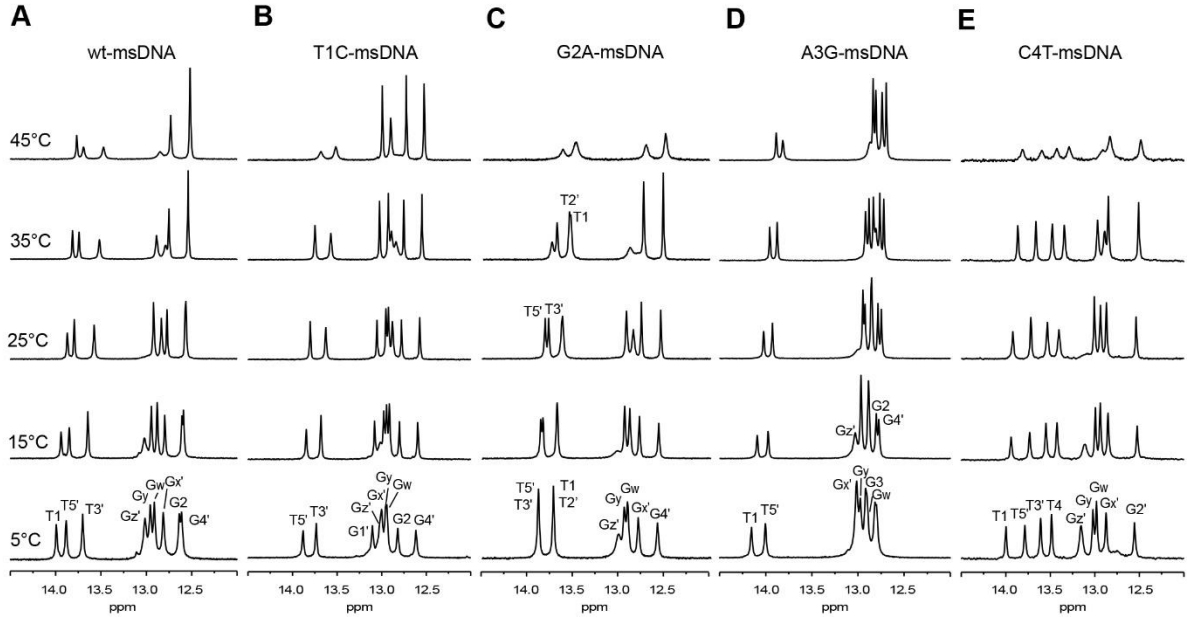

Figure 3. Temperature dependence of the imino proton resonances of the ^{1}H-NMR spectra for the wt-, T1C-, G2A-, A3G-, and C4T-msDNA duplexes. The experimental temperatures are shown on the left of each spectrum.

5 ℃. In the wt-msDNA duplex, The Gw imino proton resonance was broadened at 25 ℃ and then disappeared as temperature was increased up to 35 ℃, indicating instability of the Gw·Cw' base pair (Fig. 3). As the temperature increased, the G2 and G4' imino protons combined to appear sharp. Most imino proton resonances except the terminal Gw and Gy were observed up to 45 ℃, indicating that the wt-msDNA duplex is relatively stable at below 45 ℃. T1C-msDNA duplex spectra observed similar to wt-msDNA duplex at various temperature. However, all imino proton resonance of the G2A- and C4T-msDNA duplex were more broadened than wt-msDNA duplex at 45 ℃. This means instability caused by mutations. Also, the A3G-msDNA duplex showed sharper imino proton resonance than wt-msDNA duplex at 45℃, confirming that it became more stable.

The exchange rate constants of the imino protons for the wt-msDNA duplex were determined by water magnetization transfer method at 25 ℃. Some protons show large differences in peak intensities as a function of delay time after water inversion (Fig. 4). For example, rapid exchanging imino protons such as T3' and Gw resonance show negative peaks at delay times (100 ms in Fig. 4A), whereas the G2 and G4' resonance, which is the slowest exchanging imino proton, shows still positive up to 100 ms.

To further understand the dynamic property of the MEIS1 consensus sequence DNA duplexes, the k_{ex} measurements in the three mutant msDNA duplexes were performed at 25 ℃ and then compared with those of the wt-msDNA. In the T1C-msDNA duplex, where the T1·A1' base pair is changed to C·G base pair (see Fig. 1), the peak intensity of the G1' imino proton shows smaller dependence on the delay time after selective water inversion compared to the imino proton of the wt-msDNA duplex (Fig. 4B). This leads to a 5-fold smaller k_{ex} value of the G1' imino proton than the T1 imino proton in the wt-msDNA duplex (Table 1). This demonstrates that the G-C base pair is more stable than the corresponding A·T base pair.

Hydrogen exchange rate constants of the imino protons for the G2A-msDNA duplex, where the G2-C2' base pair is changed A·T base pair (Fig. 1), were also determined at 25℃. The peak intensity of the T2' imino proton shows much larger dependence on the delay time after selective water inversion compared to the G2 imino proton of the wt-msDNA duplex (Fig.

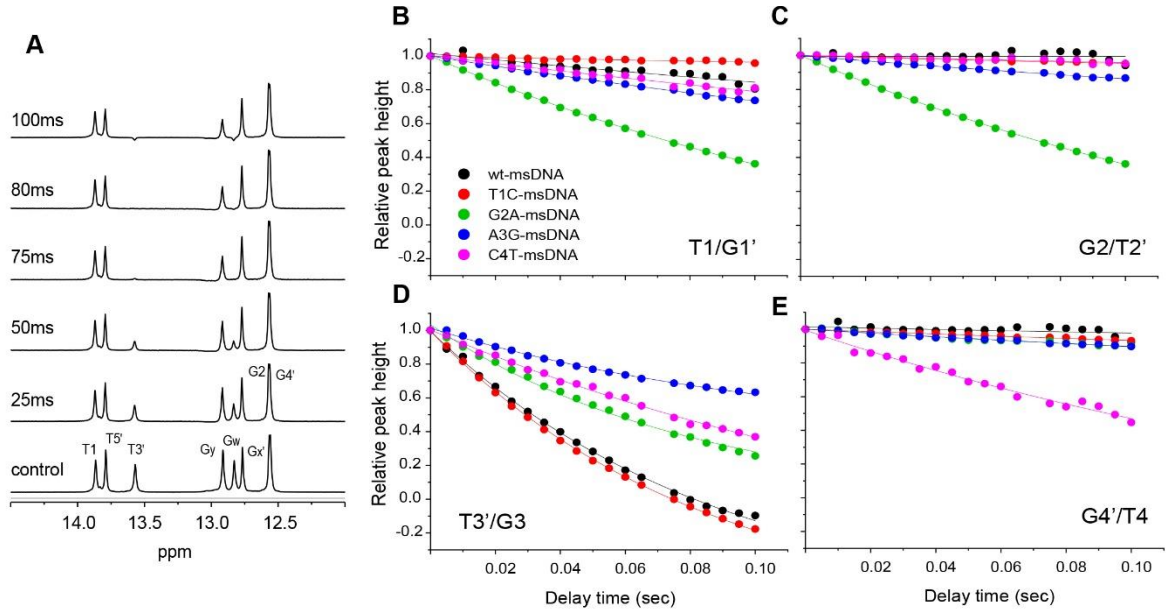

Figure 4. (A) 1D imino proton spectra of the water magnetization transfer experiments for the wt-msDNA duplex at 25 ℃. The delay times between the selective water inversion and acquisition pulse are indicated on the left of spectra. Relative peak height [I(t)/I_0] in the water magnetization transfer spectra for the (B) T1/G1', (C) G2/T2', (D) T3'/G3 and (E) G4'/T4 imino protons of the wt- (black), T1C- (red), G2A- (green), A3G- (blue) and C4T-SPL14 (triangle) duplexes as a function of delay time. Solid lines indicate the best fitting of these data using Eq. (1).

4C). This leads to a 24-fold larger k_{ex} value of the T2' imino proton than the G2 imino proton in the wt-msDNA duplex (Table 1). Surprisingly, in the G2A-msDNA duplex, the relative instability of the A2·T2' base pair induces the thermal stability of the neighboring A3·T3' base pair and the k_{ex} for the T3' imino proton has 1.5-fold smaller than of wt-msDNA duplex (Fig. 4D). In addition, the k_{ex} values of T1 imino proton could not be determined exactly because its resonance overlapped with T2' imino resonances (Fig. 3C).

Hydrogen exchange experiments were also performed at 25 ℃ for the A3G-msDNA, where A3·T3' base pair is mutated G·C base pair (Fig. 1). In the A3G-msDNA duplex, the G3 imino proton has 3-fold smaller k_{ex} value than the T3' imino proton of the wt-msDNA (Fig. 4D and Table 1). On the other hand, In the C4T-msDNA duplex, the T4 imino proton has 18-fold larger k_{ex} value than the G4' imino proton of the wt-msDNA (Fig. 4E and Table 1). Interestingly, the peak intensity of the neighboring T3' imino proton showed a weaker dependence on the delay time compared to the wt-msDNA duplex (Fig. 4D), leading to a 2.4-fold smaller k_{ex} value of the T3' imino proton than that of the wt-msDNA duplex (Table 1).

We suggest that the unique dynamic features of the four base pairs in the consensus [5'-TGAC-3'] sequence might play crucial roles in the effective DNA binding of the MEIS1 protein. In summary, we determined the k_{ex} values of the imino protons in the wild-type consensus DNA sequence as well as the mutant DNA duplexes using NMR spectroscopy. The T1C-msDNA duplex has no significant effects on the hydrogen exchange properties of the four consensus base pairs at the position 1-4 on one side of this substitution. However, the G2A-, A3G- and C4T-msDNA duplexes lead to clear changes in thermal stabilities of these four consensus base pairs. These unique dynamic features of the four base pairs in the consensus 5'-TGAC-3' sequence might play crucial roles in the effective DNA binding of the MEIS1 protein. Thus, this hydrogen exchange study can explain why the four conversed base pairs of the MEIS1 binding site are very sensitive to substitution.

Table 1. Hydrogen exchange rate constants, k_{ex} (s^{-1}) of the imino proton for the wt-, T1C-, G2A-. A3G-, C4T- msDNA duplexes at 25 ℃

Imino	wt	T1C	G2A	A3G	C4T
Gw	13.2 ± 0.03	15.5 ± 0.03	52.3 ± 0.60	6.77 ± 0.07	9.74 ± 0.04
Gx'	0.63 ± 0.03	1.32 ± 0.02	1.36 ± 0.01	3.76 ± 0.01	0.98 ± 0.07
T1/G1'	0.78 ± 0.05	0.16 ± 0.01	3.81 ± 0.01[b]	1.29 ± 0.01	0.94 ± 0.03
G2/T2'	0.16 ± 0.07[a]	0.20 ± 0.01	3.81 ± 0.01[b]	0.70 ± 0.01	0.19 ± 0.03
T3'/G3	8.94 ± 0.04	9.63 ± 0.02	6.10 ± 0.06	2.78 ± 0.03	3.73 ± 0.04
G4'/T4	0.16 ± 0.07[a]	0.30 ± 0.01	0.48 ± 0.02	0.50 ± 0.01	2.92 ± 0.07
T5'	1.95 ± 0.01	2.82 ± 0.01	4.75 ± 0.02	1.76 ± 0.01	2.21 ± 0.07
Gy	4.67 ±0.02	6.73 ± 0.02	23.1 ± 0.07	0.54 ± 0.02	4.02 ± 0.04

a. The G2 and G4' resonances in the wt-msDNA overlap. b. The T1 and T2' resonances in the G2A-msDNA overlap.

Acknowledgements

This work was supported by grants from the National Research Foundation of Korea (2020R1A2C1006909) and the Samsung Science and Technology Foundation (SSTF-BA1701-10)

References

1. J. J. Moskow, F. Bullrich, K. Huebner and I. O. Daar, *Mol. Cell. Biol,* **15,** 5434 (1995)
2. T. Nakamura, N. A. Jenkins and N.G. Copeland. *Oncogene*, **13**, 2235 (1996).
3. A. M. Buchberg, H. G. Bedigian, N. A. Jenkins and N. G. Copeland. *Mol. Cell. Biol*, **10**, 4658 (1990).
4. T. Nakamura, D. A. Largaespada, J.D. Shaughnessy and N. A. Jenkins, *Nat. Genet*, **12**, 149. (1996)
5. A. P. G Crijns, P. de Graeff, D. Geerts and K. A. Ten Hoor, *Eur. J. Cancer. Oxf. Engl. 1990*, **43**, 2495 (2007)
6. T. A. Jones, R. H. Flomen, G. Senger and D. Nizetic, *Eur. J. Cancer. Oxf. Engl. 1990* **36**, 2368 (2000)
7. J. A. Rosales-Avina, J. Torres-Flores, A. Aguilar-Lemarroy and C. Gurrola-Dıaz, *J. Exp. Clin. Cancer. Res.* **30**, 1 (2011)
8. T. R. Burglin and M. Affolter. *Chromosoma*, **125**, 497 (2016)
9. E. Bertolino, B. Reimund, D. Wildt-Perinic and R. G. Clerc. *J. Biol. Chem*, **270**, 31178 (1995)
10. A. Jolma, Y. Yin, K. R. Nitta, K. Dave, A. Popov, M. Taipale, M. Enge, T. Kivioja, E. Morgunova and J Taipale. *Nature*. **527**, 384 (2015)
11. F. Delaglio, S. Grzesiek, G. W. Vuister, G. Zhu, J. Pfeifer and A. Bax, *J. Biomol. NMR* **6**, 277. (1995).
12. W. Lee, M. Tonelli and J. L. Markley. *Bioinformatics*, **31**, 1325 (2015)
13. J.-H. Lee and A. Pardi. *Nucleic Acids Res*. **35**, 2965. (2007).
14. Y.-G. Choi, H.-E. Kim and J.-H. Lee. *J. Korean Magn. Reson. Soc*. **17**, 76. (2013).
15. H.-E. Kim, Y.-G. Choi, A.-R. Lee, Y.-J. Seo, M.-Y. Kwon and J.-H. Lee. *J. Korean Magn. Reson. Soc*. **18**, 52 (2014)